2004

MMI Devices with Weak Guiding Designed in Three Dimensions Using a Genetic Algorithm

Brian R. West
Wilfrid Laurier University, bwest@wlu.ca

Seppo Honkanen
University of Arizona

MMI devices with weak guiding designed in three dimensions using a genetic algorithm

Brian R. West and Seppo Honkanen

Optical Sciences Center, The University of Arizona, 1630 E. University Blvd., Tucson, AZ, 85721-0094
bwest@optics.arizona.edu

Abstract: We discuss the design of weakly guided multimode interference (MMI) devices using a genetic algorithm. For devices exhibiting a non-negligible vertical waveguide offset, such as those produced using ion exchange in glass, three-dimensional modeling is required to properly evaluate the device performance. A combination of semivectorial finite difference modeling in two transverse dimensions and mode propagation analysis (MPA) in the propagation direction is used to evaluate the merit of each trial design. An example is provided of a 1 x 4 power splitter designed for ion exchange, which shows considerable improvement over that obtained by self-imaging theory.

OCIS Codes: (130.3120) Integrated optics devices; (230.7370) Waveguides

References and links

1. L.H. Spiekman, Y.S.Oei, E.G. Metaal, F.H. Green, I. Moerman, and M.K. Smit, "Extremely small multimode interference couplers and ultrashort bends on InP by deep etching," IEEE Photon. Technol. Lett. **6**, 1008-1010 (1994).
2. T. Rasmussen, J.K. Rasmussen, and J.H. Povlsen, "Design and performance evaluation of 1-by-64 multimode interference power splitter for optical communications," J. Lightwave Technol. **13**, 2069-2074 (1995).
3. A. Bakhtazad, J.N. McMullin, C.J. Haugen, and R.G. DeCorby, "MMI multiplexer for dual-channel erbium-doped waveguide amplifiers," Opt. Express **9**, 178-183 (2001), http://www.opticsexpress.org/abstract.cfm?uri=OPEX-9-4-178.
4. D. Hah, E. Yoon, and S. Hong, "An optomechanical pressure sensor using multimode interference couplers with polymer waveguides on a thin p^+-Si membrane," Sens. Act. A **79**, 204-210 (2000).
5. A. Irace and G. Breglio, "All-silicon optical temperature sensor based on multi-mode interference," Opt. Express **11**, 2807-2812 (2003), http://www.opticsexpress.org/abstract.cfm?URI=OPEX-11-22-2807.
6. P.A. Besse, M. Bachmann, H. Melchior, L.B. Soldano, and M.K. Smit, "Optical bandwidth and fabrication tolerances of multimode interference couplers," J. Lightwave Technol. **12**, 1004-1009 (1994).
7. L.B. Soldano and E.C.M. Pennings, "Optical multi-mode interference devices based on self-imaging: principles and applications," J. Lightwave Technol. **13**, 615-627 (1995).
8. S.E. Yliniemi, B.R. West, T.T. Aalto, P. Madasamy, N. Peyghambarian, and S. Honkanen, "Buried ion-exchanged glass waveguides featuring low birefringence with a broad range of waveguide widths," in *Integrated Optics and Photonic Integrated Circuits*, G. C. Righini and S. Honkanen, eds., Proc. SPIE **5451**, no. 87 (2004).
9. D.F. Geraghty, D. Provenzano, M.M. Morrell, J. Ingenhoff, B. Drapp, S. Honkanen, A. Yariv, and N. Peyghambarian, "Polarisation-independent Bragg gratings in ion-exchanged glass channel waveguides," Elect. Lett. **36**, 531-532 (2000).
10. P. Madasamy, B.R. West, M.M. Morrell, D.F. Geraghty, S. Honkanen, and N. Peyghambarian, "Buried ion-exchanged glass waveguides: Burial-depth dependence on the waveguide width," Opt. Lett. **28**, 1132-1134 (2003).
11. Q. Wang, J. Lu, and S. He, "Optimal design of a multimode interference coupler using a genetic algorithm," Opt. Comm. **209**, 131-136 (2002).
12. R. Ulrich and T. Kamiya, "Resolution of self-images in planar optical waveguides," J. Opt. Soc. Amer. **68**, 583-592 (1978).
13. A.R. Gupta, "Optimization of access waveguide width of multimode interference (MMI) couplers," Opt. Commun. **221**, 99-103 (2003).

#4048 - $15.00 US Received 18 March 2004; revised 2 June 2004; accepted 3 June 2004

14. B.R. West, P. Madasamy, N. Peyghambarian, and S. Honkanen, Optical Sciences Center, The University of Arizona, 1630 E. University Blvd., Tucson, AZ, 85721, are preparing a manuscript to be called "Accurate modeling of ion-exchanged glass waveguide structures."
15. C. M. Kim and R. V. Ramaswamy, "Modeling of graded-index channel waveguides using nonuniform finite difference method," J. Lightwave Technol. **7**, 1581-1589 (1989).
16. J. Leuthold, J. Eckner, E. Gamper, P.A. Besse, and H. Melchior, "Multimode interference couplers for the conversion and combining of zero- and first-order modes," J. Lightwave Technol. **16**, 1228-1239 (1998).

1. Introduction

Planar waveguide multimode interference (MMI) devices have found numerous applications in telecommunications [1-3] and sensing [4,5], owing to their compactness, high fabrication tolerance, and wide optical bandwidth [6]. As the operation of the MMI relies on a quadratic distribution of modal effective indices in the multimode section [7], conventional thought is that waveguides exhibiting weak guiding cannot produce efficient MMI devices. As several material systems used for integrated optics do result in weak guiding, it is important to investigate the resultant changes in design procedures.

One particular technology that has recently found commercial applications is ion exchange in glass. Ion-exchanged waveguides exhibit low propagation loss and compatibility with single-mode fiber, and cost relatively little to produce. In addition, very low birefringence is possible across a wide range of waveguide widths [8], resulting in devices that show very low polarization dependent loss [9]. It has been shown [10] that when the ionic species being exchanged have substantially different mobilities, the depth of the waveguide after burial is dependent upon the waveguide width. This will have an adverse effect upon MMI devices, which contain transitions between narrow access guides and the multimode section. Proper analysis of these transitions requires that both vertical and transverse field variations be modeled. Such an approach is unique to MMI design, as most authors prefer to eliminate vertical field variation through such techniques as the effective index method.

Section 2 of this paper reviews the design of an MMI 1 x *N* power splitter using self-imaging theory. In section 3, we discuss the challenges posed by using a weakly guided multimode section, with particular emphasis on those fabricated by ion exchange, and their effects on the results of self-imaging theory. We then propose, in section 4, an alternate design procedure using a genetic algorithm (GA). This algorithm is used in section 5 to design a 1 x 4 power splitter in ion exchange, and it is shown that polarization dependent loss and power imbalance in the output waveguides can be essentially eliminated in the design. A previous effort to use a GA for MMI optimization has been reported [11]. This procedure differs considerably from that reported in the present text in that the variation of mode fields in the vertical direction is not accounted for, and that the position of each access waveguide is related through an effective MMI width. Both of these approximations lose validity in the case of ion exchanged waveguides.

2. Self-imaging theory of multimode interference

For a strongly guided, step-index multimode waveguide, it can be assumed that the penetration depth of each transverse mode into the cladding is equal and negligible. Thus, within the paraxial approximation, the distribution of propagation constants β_v is quadratic,

$$(\beta_0 - \beta_v) \cong \frac{v(v+2)\pi}{3L_\pi}, \tag{1}$$

#4048 - $15.00 US Received 18 March 2004; revised 2 June 2004; accepted 3 June 2004

where v is the mode number and $L_\pi = \pi / (\beta_0 - \beta_1)$ is the "beat length" between the two lowest-order modes [7]. At the input to the multimode section, the field distribution of the input access waveguide can be expanded in the eigenmodes of the multimode guide,

$$\Psi(x, y, z = 0) = \sum_v a_v \varphi_v(x, y) , \tag{2}$$

where the a_v are the expansion coefficients, calculated using the overlap integrals

$$a_v = \frac{\iint \Psi(x, y, z = 0) \varphi_v(x, y)\, dx\, dy}{\sqrt{\iint \varphi_v^2(x, y)\, dx\, dy}} . \tag{3}$$

The summation is over all guided and leaky modes, although the latter may be neglected in all practical cases, as their a_v are relatively small for practical access waveguide widths. As each mode propagates in z, it accumulates a phase term equal to $\exp(-i \beta_v z)$. Using Eq. (1), we find that the field distribution at the output plane of the multimode guide is

$$\Psi(x, y, z) = \sum_v a_v \varphi_v(x, y) \exp\left(i \frac{v(v+2)\pi z}{3L_\pi} \right), \tag{4}$$

where a global phase factor has been omitted. The application of Eqs. (2) - (4) is commonly referred to as Mode Propagation Analysis (MPA). If the input access waveguide is symmetric with the multimode section, analysis of Eq. (4) shows that the shortest N-fold self-imaging distance is

$$L_{MMI} = \frac{3L_\pi}{4N} \tag{5}$$

from the input [7]. A 1 x N power splitter is shown in Fig. 1.

The output access waveguides are equally spaced and arranged symmetrically about the axis of the multimode waveguide. The x-coordinate of the center of the i^{th} waveguide is then

$$x_i = \frac{(2i - (N+1))}{2N} W_e , \tag{6}$$

where W_e is the effective width of the multimode waveguide, equal to the physical width in the strongly guided case.

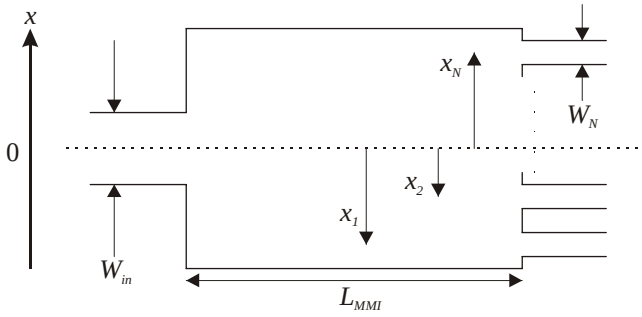

Fig. 1. Layout of a 1 x N power splitter, showing geometrical parameters.

#4048 - $15.00 US
Received 18 March 2004; revised 2 June 2004; accepted 3 June 2004

The optimal width of the input access guide is somewhat difficult to determine. A waveguide that is too wide will not excite enough transverse modes of the multimode section (as a general rule, for a 1 x N splitter, at least $N + 1$ guided modes must be excited in the multimode waveguide in order to resolve the desired output field [12]). On the other hand, too narrow a guide will launch more power into the substrate modes of the multimode section, increasing the excess loss of the device. The optimal width of the output waveguide has been the subject of previous study [13], and can be estimated as the widest guide that exhibits negligible coupling to adjacent guides.

3. Weakly guided MMI devices

When the index difference between core and cladding in the multimode guide is small or contains a gradient as with diffused waveguides, higher-order transverse modes have greater effective widths. As a result, the distribution of effective indices is sub-parabolic, as can be inferred from [7]. The gradual de-phasing of the modes during propagation will blur the self-images and produce both a longitudinal and transverse shift in the optimal locations of the output waveguides. In addition, the width of the multiple self-images shows a slight increase as distance from the axis of symmetry increases.

Determining the optimum access waveguide width for buried ion-exchanged MMI devices is quite difficult, due to the vertical offset between waveguides of dissimilar width [10]. Generally speaking, the widths need to be increased in order to balance transverse resolution against vertical insertion loss.

4. Description of the genetic algorithm

The GA described in this paper seeks the best MMI design by simultaneously optimizing several geometrical parameters. It is assumed that the fabrication process and width of the MMI section are pre-determined. Referring to Fig. 1, the parameters to be determined are the length of the MMI section (L_{MMI}), width of the input guide (W_{in}), and positions (x_i) and widths (W_i) of the output guides. By symmetry, many of these parameters can be eliminated; for N even, only $N / 2$ positions and $N / 2$ widths need be determined, while for N odd, $(N - 1) / 2$ positions and $(N + 1) / 2$ widths are required, for a total of $N + 2$ parameters in total.

Before the GA begins, a library is created containing the quasi-TE and -TM mode fields for all possible access waveguide widths (in increments of 0.1 μm) as well as the fields and propagation constants β_v of the multimode waveguide. Modeling of the ion exchange process is described in [14], and a semivectorial finite difference method described in [15] is used to solve for all eigenmodes and propagation constants. This is done to eliminate the need to perform process modeling or optical mode solution of every waveguide during execution of the GA. The absence of such modeling within each generation of the GA drastically reduces the computational effort required to optimize the device design. Note that the process modeling is performed only in transverse slices. Strictly speaking, this does not account for longitudinal ion diffusion at the transition regions, but this effect exists over a distance of only a few microns. As such, there will be no appreciable adiabatic tapering, and perhaps a very slight improvement in power coupling. The 0.1 μm resolution in guide width reflects the finite lithographic precision. Next, the power in the multimode section for an arbitrary symmetric input is calculated over a coarse grid using Eqs. (2)-(4), and plotted as in Fig. 2, in order to estimate the optimum device length to within a few tens of microns.

Each of the $N + 2$ parameter ranges is binary-encoded to arbitrary precision in a "gene" (as above, the practical limit of precision is on the order of 0.1 μm). The genes are concatenated to form a "chromosome." In this way, all geometrical parameters to be optimized are encoded in a single binary sequence. For the waveguide widths, the value encoded in the gene is rounded to the nearest 0.1 μm, in order to utilize the pre-computed mode field libraries. Other parameters are not rounded off in the GA, but are only quoted to the nearest 0.1 μm in this paper.

#4048 - $15.00 US Received 18 March 2004; revised 2 June 2004; accepted 3 June 2004

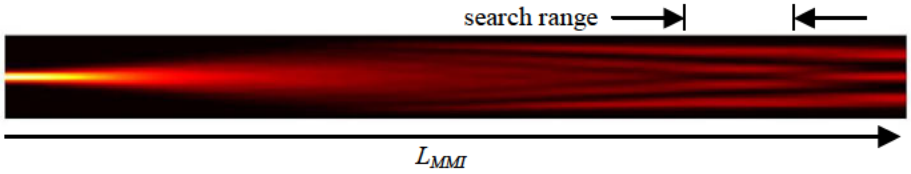

Fig. 2. Power in the multimode waveguide, showing region of 1 x 4 splitting.

An initial population of trial devices is randomly generated, and modeled using Eqs. (2)-(4) for both polarizations. Power coupled into each output waveguide is calculated using an overlap integral with the fundamental mode of the output waveguide, shifted to the appropriate transverse position. Power coupled into any higher-order modes of the output waveguides will be radiated during the down-taper to a single mode output, and therefore is not considered here. Similarly, it is assumed that only the fundamental mode of the input waveguide is present; this can be achieved by an adiabatic up-taper. In this paper, care is taken to ensure that evanescent coupling between the output waveguides is negligible. If this is not the case, techniques such as beam propagation method (BPM) can be applied to propagate the output fields through diverging waveguides.

If, for unit input power, the power coupled to the i^{th} output waveguide is P_i, and the total TE and TM output power is P_{TE} and P_{TM}, respectively, we can define three properties of the modeled device, all in dB:

$$XL = -10\log_{10}(\sum_{i=1}^{N} P_i) \quad \text{(excess loss)}, \tag{7}$$

$$IB = -10\log_{10}(P_i^{\min} / P_i^{\max}) \quad \text{(imbalance)}, \tag{8}$$

$$PDL = -10\log_{10}(P_{pol}^{\min} / P_{pol}^{\max}) \quad \text{(polarization dependent loss)}. \tag{9}$$

Here, $P_i^{\min}$ ($P_i^{\max}$) is the smallest (largest) P_i, and $P_{pol}^{\min}$ ($P_{pol}^{\max}$) is the smaller (larger) of P_{TE} and P_{TM}.

A figure of merit is determined for each trial device,

$$F = \exp[-(C_{XL}XL + C_{IB}IB + C_{PDL}PDL)], \tag{10}$$

where the C_j are weighting coefficients that determine the relative importance of each property. If all of the F are below a target value, a subsequent generation of trial devices is created, where the probability of a chromosome becoming a "parent" is proportional to its value of F. A single-point crossover of the two parent chromosomes is used, and a small but finite probability of single-bit "mutation" ($0 \rightarrow 1$ or $1 \rightarrow 0$) is applied in order to escape local maxima of F in parameter space. Successive generations of devices are modeled until the target figure of merit is achieved. As it is common in GAs for well-evolved generations to contain multiple identical chromosomes, each value of F is recorded in order to avoid redundant calculations.

5. Example

We examined the design of a 1 x 4 splitter, with a mask opening width of 40 μm in the multimode section. The guide supports 9 guided modes at 1.55 μm in both TE and TM

#4048 - $15.00 US
Received 18 March 2004; revised 2 June 2004; accepted 3 June 2004

polarization, with effective indices as shown in Table 1. The splitter is designed first by using the calculated β_0 and β_1 (averaged over polarization), and Eqs. (1)-(6). Modeling shows a very poor excess loss of 2.088 dB, an imbalance of 1.225 dB, and a polarization dependent loss of 0.016 dB (note that this particular ion exchange process inherently exhibits very low birefringence). The results are summarized in Table 2.

Next, we use the GA to design the same device. As mentioned in Section 4, we are free to choose the relative importance of each device property. For this example, we assume that the device application requires as small a power imbalance and polarization dependent loss as possible, with less strict requirements on excess loss. In this case, we set $C_{XL} = 0.5$, $C_{IB} = 1$, and $C_{PDL} = 10$. The search ranges and resolution of each parameter are shown in Table 3. After 250 generations with 15 trial devices per generation, the GA converged to the parameters shown in Table 2. The imbalance is 0.007 dB, and polarization dependent loss is 0.001 dB. Excess loss is 1.901 dB, dominated by the vertical mismatch at the output plane.

Figure 3 contains simulated TE power cross-sections of the end of the multimode guide using self-imaging theory (top) and the GA (bottom), showing a significant improvement in the latter. Comparing Fig. 3 and Table 2, it can be seen that, although the outermost of the four self-images are higher in power, imbalance is minimized by an intentional transverse misalignment of the output waveguides. The excess loss due to this misalignment is ≈ 0.5 dB, producing a total excess loss for the GA-designed device that is still lower than that of the self-imaging theory design.

Table 1. Simulated effective indices of guided modes in the multimode waveguide

Mode number	n_{eff} (TE)	n_{eff} (TM)
0	1.46163	1.46154
1	1.46126	1.46117
2	1.46065	1.46056
3	1.45981	1.45973
4	1.45877	1.45868
5	1.45755	1.45746
6	1.45616	1.45607
7	1.45462	1.45453
8	1.45296	1.45287

Table 2. Results of self-imaging theory and genetic algorithm

Parameter	Self-imaging	GA
L_{MMI} (μm)	395.7	446.7
W_{in} (μm)	10.0	11.3
W_1 (μm)	5.0	6.0
W_2 (μm)	5.0	4.5
x_1 (μm)	5.0	6.6
x_2 (μm)	15.0	15.1
Excess loss (dB)	2.088	1.901
Power imbalance (dB)	1.225	0.007
PDL (dB)	0.016	0.001
Simulations per generation	N/A	15
Generations	N/A	250

#4048 - $15.00 US Received 18 March 2004; revised 2 June 2004; accepted 3 June 2004

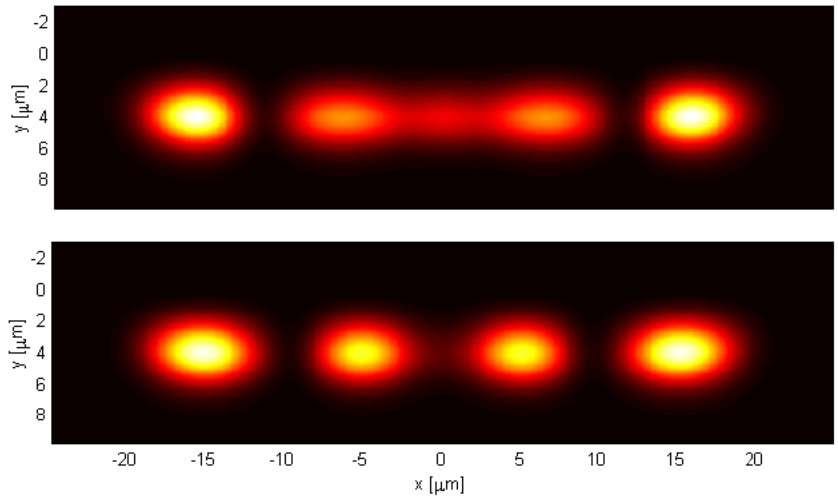

Fig. 3. Power cross-sections at the output plane of the MMI, designed using self-imaging (top) and genetic algorithm (bottom). While the inner and outer power peaks are of different magnitude, minimization of power imbalance is achieved through an intentional transverse offset of the output waveguides.

Table 3. Parameters used in the genetic algorithm

Parameter	L_{MMI}	W_{in}	W_i	x_i
Range (μm)	400-500	2-14	2-6	$x_i^* \pm 2$ [a]
Resolution (bits)	10	7	6	6

[a] x_i^* is the value of x_i calculated using Eq. (6)

6. Conclusions

A genetic algorithm was used to determine the design parameters of an ion-exchanged 1 x 4 power splitter. Modeling of the GA-designed device exhibited considerable improvements over that designed using self-imaging theory in terms of excess loss, power imbalance, and polarization dependent loss. The concepts developed in this paper are expected to have even greater significance when designing more complicated devices, such as mode converters [16] and tap couplers, for which no analytical design rules are known. Furthermore, it is possible to incorporate additional terms into the figure of merit, such as the phase relations between each of the output images. This would extend the utility of the GA to such devices as generalized Mach-Zehnder switches and phase-diversity receivers.

While the GA of this paper uses mode propagation analysis to simulate each trial device, other numerical methods, such as BPM, would improve simulation accuracy. However, given the large number of devices required to simulate in three dimensions for the GA, considerable computational resources would be necessary.

#4048 - $15.00 US
Received 18 March 2004; revised 2 June 2004; accepted 3 June 2004